PERGAMON

International Journal of Multiphase Flow 25 (1999) 1195–1223

International Journal of Multiphase Flow

www.elsevier.com/locate/ijmulflow

Influence of Froude number on physical processes determining frequency of slugging in horizontal gas–liquid flows

Bennett D. Woods, Thomas J. Hanratty*

Department of Chemical Engineering University of Illinois, Urbana, IL 61801, USA

Received 7 July 1998; received in revised form 10 May 1999

The authors are pleased that this article is part of a volume honoring Professor Gad Hetsroni. His efforts to advance the field of multiphase flows are gratefully acknowledged.

Abstract

The effect of the liquid Froude number on the physical processes for forming slugs was investigated for cocurrent air–water flow through a 7.63 cm horizontal pipeline that was 20 m long. The transient characteristics are described by using simultaneous measurements of the liquid holdup at multiple locations. When the Froude number of the stratified flow at the onset of slugging is less than unity, the frequency is related to the propagation, upstream of gravity waves caused by the formation of slugs. A stochastic model is used to describe the formation for Froude numbers greater than unity. These results provide a physical basis for developing models for the frequency of slugging. © 1999 Elsevier Science Ltd. All rights reserved.

Keywords: Gas–liquid pipe flow; Slug flow; Slug frequency

1. Introduction

The slug flow pattern, observed in horizontal pipes, is characterized by the intermittent appearance of aerated masses of liquid that travel downstream approximately at the local gas velocity. These slugs are separated from one another by a stratified configuration that contains

* Corresponding author. Tel.: +1-217-333-1318; fax: +1-217-333-5052.
E-mail address: hanratty@scs.uiuc.edu (T.J. Hanratty)

PII: S0301-9322(99)00058-0

a slower moving liquid layer. Dukler and Hubbard (1975) developed a model for predicting the pressure drop and liquid holdup by assuming that slug flow can be represented by a sequence of identical units translating at a constant velocity. This idea has been used in subsequent works by Nicholson et al. (1978), Kokal and Stanislav (1989) and Andreussi et al. (1993). A critical issue in developing these models is the prediction of the slug frequency or the slug length.

Slug lengths have been reported to be in the range of 12–30D for horizontal air–water flow (Dukler and Hubbard, 1975; Nicholson et al., 1978; Nydal et al., 1992). Taitel et al. (1980) and Dukler et al. (1985) recognized that new liquid is scooped up into the body of the slug from the slower moving liquid layer and suggested that the minimum stable slug length is determined by the distance required to establish a fully turbulent velocity profile.

Taitel and Dukler (1977) introduced the notion that slug frequency is related to events that occur in the beginning portion of the pipeline, where slugs form from interfacial disturbances. They observed that the initiation of a slug is associated with the depletion of liquid in the slug formation zone and argued that the frequency of slugging is given by the time required to rebuild the liquid from a level required to initiate slugs, h_s, to the height of the liquid layer, h_e, in a fully developed stratified flow at the same gas and liquid flow rates. Tronconi (1990) used linear stability theory and the concept of a 'most dangerous wave' proposed by Mishima and Ishii (1980) to identify the frequency of the unstable wave responsible for initiating a slug.

Hubbard (1965), Gregory and Scott (1969) and Heywood and Richardson (1979) examined the effect of gas and liquid flow rates on the frequency of slugging. All of these investigators reported a minimum in the frequency at a superficial gas velocity of about 4 m/s for the range of conditions that they studied. This result is consistent with observations of air–water flow in a 9.53 cm pipe at atmospheric pressure by Lin and Hanratty (1986a, 1986b), Fan et al. (1993a, 1993b) and Andritsos et al. (1989), that the wave patterns and the mechanism of slug formation are different for large and small gas velocities. Below 4 m/s, they found that slugs evolve from regular gravity waves which grow and eventually bifurcate as they propagate downstream. If the average height of the liquid layer is greater than a certain value, h_s, the bifurcated waves can form a slug. Above 4 m/s, they found that irregular waves appear in a stratified flow. If the liquid layer is thick enough, the waves can coalesce and form a slug. These considerations, plus the recognition that the design of the gas–liquid mixer at the entry could affect slug formation suggest, that it may not be possible to describe the frequency of slugging with a single mechanism.

This paper provides a detailed account of the physical processes that determine the frequency of slugging, defined as the number of slugs passing a stationary observer per unit time. The system considered is water and air flowing in a 7.63 cm horizontal pipe. The evolution of slugs was studied by measuring the liquid holdup at a number of locations along a 20 m length. These studies reveal that the mechanisms responsible for the formation of a slug, and thus the slug frequency, depend on the liquid Froude number of the wavy stratified flow, the gas velocity, and the location in the pipeline at which the slugs form. The results do not support the proposals by Taitel and Dukler (1977) and by Tronconi (1990).

Film heights defining the transition from stratified to slug flow, h_s, and the necessary height for the stability of a slug, h_o, are important parameters needed to interpret the results. Ruder

et al. (1988) have shown that h_s is greater than h_o for air–water flow at low gas velocities and atmospheric pressure. Therefore, an instability at the gas–liquid stratified interface has the possibility of creating a stable slug. Ruder et al. (1988), Bendikson and Esperal (1992) and Woods and Hanratty (1996) point out that for large enough gas densities, h_o is greater than h_s, so the stability of a slug, rather than a stratified flow determines the initiation of slug flow.

2. Background

2.1. Stability of a stratified flow

The classical inviscid linear analysis of the stability of a stratified flow considers an infinitesimal wave at the interface of two fluids which, for the case considered here, are a gas with velocity U and a liquid with velocity u. The following relation is derived between the wave velocity, C, and the wavenumber, $k = 2\pi/\lambda$, (Milne-Thomson, 1968):

$$k\rho_L(u-C)^2\coth kh + k\rho_G(U-C)^2\coth kH = g(\rho_L-\rho_G)+\sigma k^2. \tag{1}$$

Here, H is the height of the gas layer, h, the height of the liquid layer, ρ_G, the gas density ρ_L, the liquid density, g, the acceleration of gravity, and σ, the surface tension. Instability is defined by a complex or imaginary value of C. This occurs when the destabilizing effects of liquid inertia and gas phase pressure variations 180° out of phase with the wave profile are larger than the stabilizing effects of gravity and surface tension. If one considers long wavelength waves, for which $kh \ll 1$ and $kH \ll 1$, and if ρ_G/ρ_L is small, (1) predicts the following relations for the initiation of an instability:

$$\rho_G(U-u)^2 = \rho_L gH, \tag{2}$$

$$C_R \cong u \tag{3}$$

Wallis and Dobbins (1973) and Taitel and Dukler (1976) examined whether Eqs. (2) and (3) predict the initiation of slugs. They found that (2) overpredicts the critical gas velocity by a factor of about 2. From Eqs. (3) and (1), it is seen that the inviscid analysis predicts that liquid inertia is neither stabilizing nor destabilizing. Lin and Hanratty (1986a, 1986b) and Wu et al. (1987) used a long wavelength viscous analysis that introduces the influence of a shear stress at the gas–liquid interface and a resisting stress at the wall. This yields values of C_R which are different from u and a destabilizing influence of liquid inertia. Predicted critical gas velocities are in good agreement with measurements for air–water flows, if the interfacial shear stress is taken to be twice the value for a smooth surface. The equation developed by Lin and Hanratty is used to define the values of h_s used in this paper. However, this analysis does not have general application. Eq. (2) and the analysis of Lin and Hanratty (1986a, 1986b) predict that the critical U increases with pipe diameter, in agreement with experiments with air–water flows. However, studies with liquids having viscosities greater than 20 cp (Andritsos et al., 1989) have shown no effect of pipe diameter. The transition in these cases is predicted by the classical

Kelvin–Helmholtz analysis (2) and slugs are found to evolve from capillary-gravity waves, rather than from long wavelength gravity waves.

2.2. Stability of a slug

Fig. 1 gives a pictorial representation of a slug moving over a stratified liquid layer of area A_{L1} and velocity u_1, which is assumed to contain no air bubbles. Liquid is incorporated into the front of the slug at a rate given by $(C_F - u_1)A_{L1}$, where C_F is the velocity of the front of the slug. Liquid is shed from the tail at a rate Q_L, so a necessary condition for a stable or growing slug is

$$(C_F - u_1)A_1 \geq Q_L \tag{4}$$

Ruder et al. (1988) used Eq. (4) to define a critical height, h_o (obtained from A_{L1}), by calculating Q_L with the equation for a bubble displacing liquid in a horizontal tube (Benjamin, 1968). For a stationary condition, $C_F = C_B$, they obtained

$$\frac{A_{L1}}{A} = \frac{0.542\sqrt{gD}}{C_B - u_1}, \tag{5}$$

where D is the pipe diameter. Eq. (5) has been found to define h_o in the limit of small gas velocities, for which the slug body is unaerated.

Woods and Hanratty (1996) made direct measurements of Q_L for air and water flowing in a horizontal pipe with a diameter of 0.0953 m. At high gas velocities, h_o was found to deviate from Eq. (5). The open points in Fig. 2 are calculated values of h_o. The darkened points represent the observed transition to slug flow. The solid curve is the prediction of h_s obtained by Lin and Hanratty (1986a, 1986b). At low U_{SG}, the critical height predicted by linear stability theory is greater than the height required for slug stability. At high U_{SG}, linear stability theory does not correctly predict h_s (Lin and Hanratty, 1986a, 1986b; Fan et al., 1993a, 1993b); transition is determined by the stability of slugs.

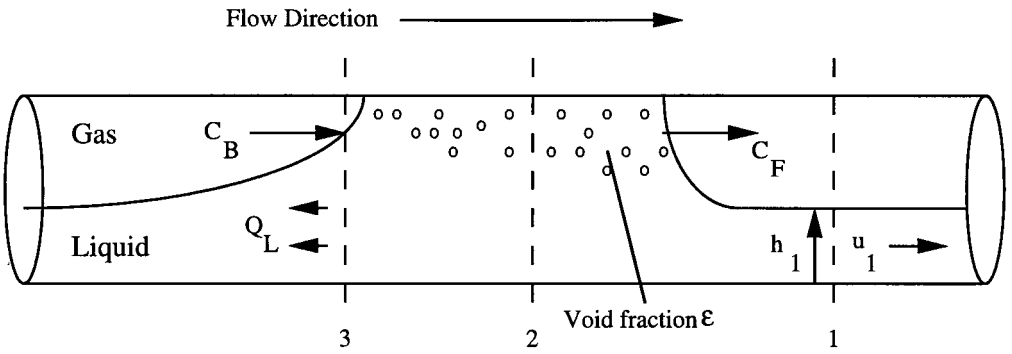

Fig. 1. Pictorial representation of a slug.

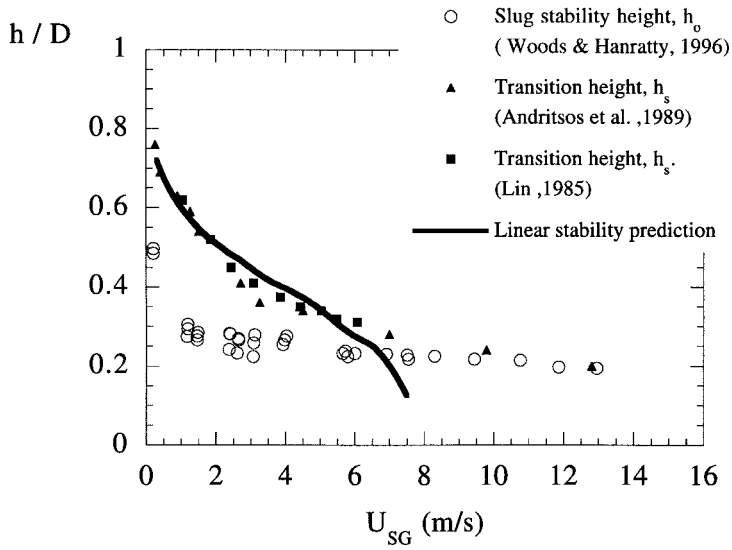

Fig. 2. Variation of h_s and h_o with U_{SG}.

2.3. Formation of slugs in subcritical flows

The formation of a slug is associated with a depletion of liquid. Replenishment occurs rapidly enough that inertia dominates. Therefore, the effects of viscosity and of the air flow can be ignored, to a first approximation. At the instant a slug appears, the liquid layer behind the slug is approximated as a discontinuity (see Fig. 3). Two means exist for rebuilding the liquid level, the flow of new liquid into the pipe and the upstream propagation of a depression (gravity) wave from the location at which a slug formed (the breaking dam problem discussed by Stoker, 1957). The relative importance of these two mechanisms can be determined by considering the propagation velocity of a long wavelength gravity wave in a stationary shallow liquid

$$C = \sqrt{gh}. \tag{6}$$

In a flowing liquid, a gravity wave that moves upstream would have a velocity

$$-C = \sqrt{gh} - u. \tag{7}$$

A consideration of Eq. (7) shows it is not possible for a depression wave to move upstream if the Froude number $Fr = u/\sqrt{gh}$, is greater than unity. In this case, the refilling will occur by a bore moving downstream.

An idealized picture of the refilling by a depression wave is depicted in Fig. 3. It is assumed that the formation of a slug at location L_D results in the fluid configuration shown in Fig. 3a. The conditions at the inlet are maintained at an approximately constant h_i and u_i by the incoming fluid. If $Fr > 1$, the discontinuity in the fluid would propagate downstream. For $Fr<1$, a wave forms from the discontinuity. One portion of the wave moves upstream with a

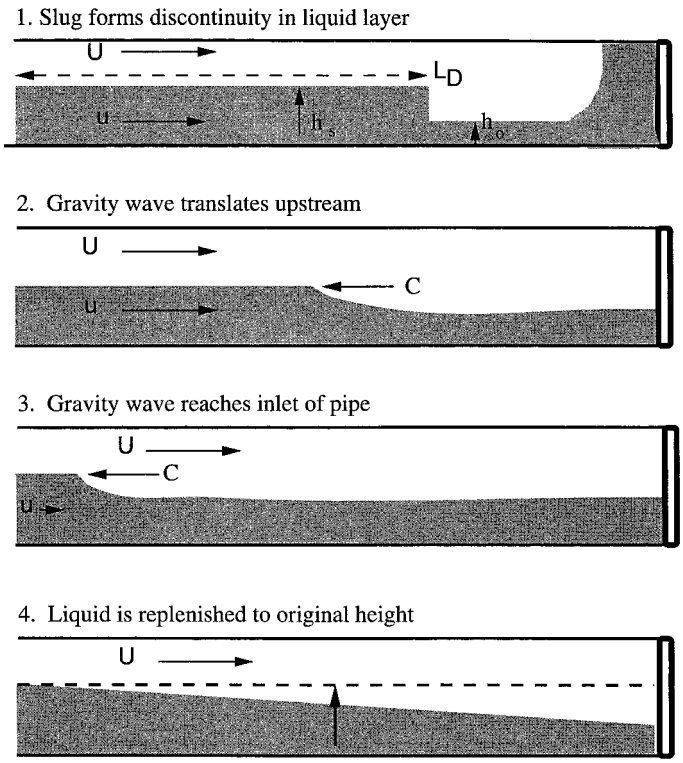

Fig. 3. Schematic of a gravity wave translating upstream after the formation of a slug.

velocity given by Eq. (7). The lower portion moves downstream. The wave which moves upstream is reflected at the inlet. As shown in Fig. 3d, the pipe is then refilled and the height of the liquid at $x = L_D$ can change.

Shallow water wave equations are used to describe the motion of the gravity wave. The mass and momentum balances are

$$\frac{\partial h}{\partial t} + u\frac{\partial h}{\partial x} + h\frac{\partial u}{\partial x} = 0 \tag{8}$$

$$\frac{\partial u}{\partial t} + u\frac{\partial u}{\partial x} + g\frac{\partial h}{\partial x} = 0 \tag{9}$$

where u is the liquid velocity, h, the height of the liquid, t, time, and x, the distance downstream. Viscous effects are not considered in Eq. (9) because in rapid transient flows they are small compared to the terms appearing in Eq. (9). Cartesian coordinates with h equal to the height of the stratified flow at the centerline of the pipe, are used as a simplification. The initial condition is a discontinuity in the liquid level at $x = L_D$. The height at the inlet needs to be slightly greater than h_s for the stratified flow to become unstable at L_D. The equations are solved to determine how the velocity and height change with space and time and, in particular,

to calculate the time required to rebuild the liquid layer at $x = L_D$ back to the height required to initiate another slug. This is taken as the interval between slugs for the case of $Fr<1$.

Eqs. (8) and (9) can be written in dimensionless form by using h_s as a characteristic length in the y-direction, L_D as a characteristic length in the x-direction, u_s as a characteristic velocity, and L_D/u_s as a characteristic time.

$$\frac{\partial h^*}{\partial t^*} + u^* \frac{\partial h^*}{\partial x^*} + h^* \frac{\partial u^*}{\partial x^*} = 0 \tag{10}$$

$$\frac{\partial u^*}{\partial t^*} + u^* \frac{\partial u^*}{\partial x^*} + \frac{1}{Fr^{*2}} \frac{\partial h^*}{\partial x^*} = 0 \tag{11}$$

$$Fr^* = \frac{u_s}{\sqrt{g h_s}} \tag{12}$$

3. Experiments

The flow facility used in this study consists of a horizontal pipeline with a diameter of 0.0763 m and a length of 23 m. The pipe segments are constructed from Plexiglas to allow visual observations of the flow conditions. The pressure is atmospheric. Both phases are combined in a tee section with the liquid in the run and the gas entering from the top. The air flow is forced through an orifice located 5 pipe diameters upstream of the tee section. The velocity of the air through this orifice approaches the local velocity of sound. Consequently, downstream variations in the gas phase pressure caused by the formation of slugs do not strongly affect the inlet air flow.

Measurements of the variation of the liquid holdup and wave properties were obtained with a liquid conductance technique. A probe, consisting of two chromel wires, traverses the diameter of the pipe vertically. When a signal is applied to one of the wires, the conductance between the two wires is dependent upon the volume fraction of liquid between the wires. Each conductance probe is calibrated to compensate for differences in construction. Conductance measurements are converted into an equivalent h/D, where h is the liquid height at the bottom of the pipe.

Pressure fluctuations associated with the passage of a slug were measured using a piezoresistive pressure transducer mounted flush with the wall. A characteristic pressure pulse reveals the passage of a slug, as described by Lin and Hanratty (1986a, 1986b), Fan et al. (1993a, 1993b). This method of identifying slugs is useful at large gas velocities where the liquid is highly aerated and large amplitude waves need to be distinguished from slugs.

Six or seven conductance probes were located at various positions along the pipeline. The probes were sampled simultaneously in order to study the transient behavior of the liquid layer. Probes located near the inlet monitor the growth of waves which are responsible for initiating slugs. The depletion and rebuilding of the liquid layer due to the intermittent formation of slugs is studied with probes located farther downstream.

4. Definition of sub-regimes

A number of sub-regimes, which are distinguished from one another by the mechanism for slug formation, are defined in Fig. 4. Curve A gives the observed transition from a wavy stratified to a slug flow. Slugs are observed to form far downstream in the pipeline for conditions close to the transition curve. As U_{SL} increases for a fixed U_{SG}, slugs form closer to the inlet. For conditions below B, slugs appear at $L/D >$ Ca. 40, so that the formation could be weakly dependent on the design of the inlet. Curve C defines when $Fr = 1$ at the inlet. Zone I in Fig. 4 is defined as the region in which $Fr<1$ and slugs form downstream of $L/D >$ Ca. 40. The region of the flow regime map in which $Fr > 1$ and slugs form at $L/D >$ Ca. 40 is defined as zone II. For high U_{SL}, slugs form upstream of $L/D =$ Ca. 40. This is denoted as zone III.

Fig. 5 shows measurements for $U_{SG} = 1.2$ m/s and $U_{SL} = 0.16$ m/s (zone I of Fig. 4). This is a condition for which the flow at the inlet is subcritical ($Fr = 0.36$, $u = 0.25$ m/s) and no slugs form at $L/D<40$. The presence of slugs at $L/D = 98$ is indicated by the peaks in h/D. From Fig. 2, one observes that h_s/D is approx 0.6. The stratified flow at the inlet is maintained at a height approximately equal to h_s (see the results for $L/D = 12$ in Fig. 5). If no slugs were present in the pipe, the stratified flow would assume an equilibrium height, h_e, which is larger than h_s. The slugs, therefore, feed information back to the inlet, through the backward moving waves, to regulate the height. The height of the stratified flow required for a stable slug to exist is found to be $h_o/D \approx 0.3$ in Fig. 2. One notes that this is a lower limit for the height of the liquid layer behind a slug. Thus, the stratified layer changes from h_s to h_o during replenishment rather than from h_e to h_s, as suggested by Taitel and Dukler (1977). The time interval over which a slug is detected at $L/D = 180$ is larger than at $L/D = 98$. This suggests that the slug is growing in length since its velocity is approximately constant. The height of the liquid in front of the slug is greater than that necessary to stabilize it, $h > h_o$. The slug grows by consuming liquid in this layer. In a much longer pipe than used in the experiments, one could presume

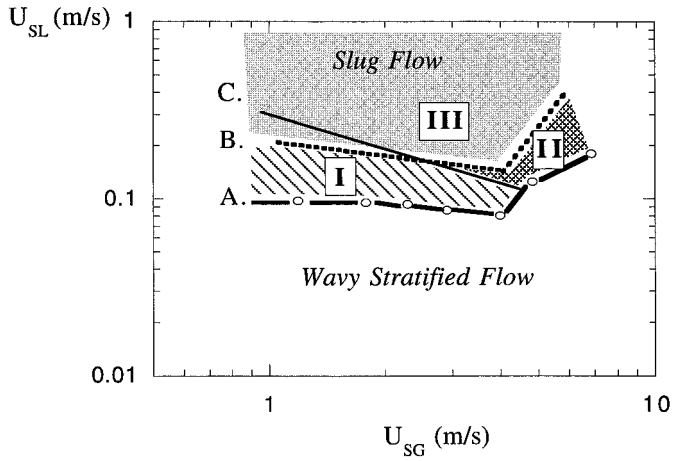

Fig. 4. Flow regime map for air–water flow in horizontal 0.0763 m pipe. Curve A indicates the transition to slug flow; between curves A and B, slugs form downstream of $L/D =$ Ca. 40; along curve C, $Fr = 1$ at the inlet.

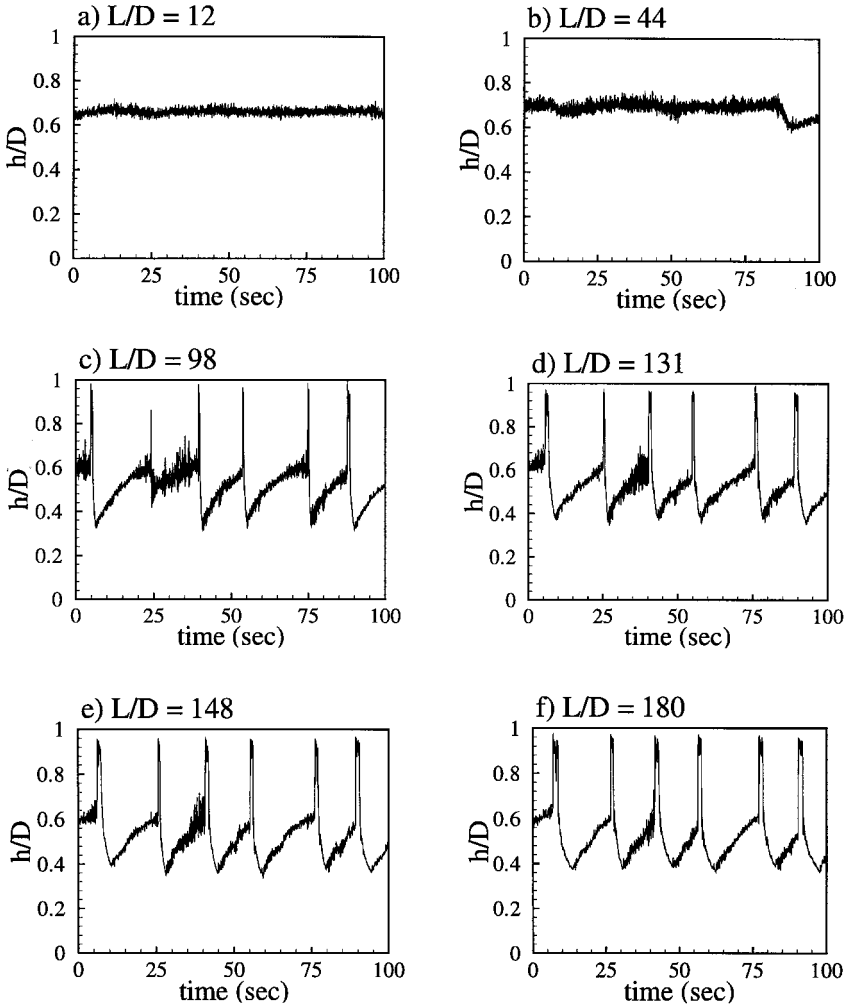

Fig. 5. Liquid holdup measurements for $U_{SG} = 1.2$ m/s, $U_{SL} = 0.16$ m/s.

that slugs stop growing (unless they coalesce) and that the stratified flow between slugs would have a value slightly greater than h_o.

Fig. 6 shows slug formation for $U_{SG} = 5.5$ m/s and $U_{SL} = 0.23$ m/s (zone II of Fig. 5). The conditions at the inlet are such that the stratified flow is supercritical, $Fr = 1.3$. Values of $h_s/D \approx 0.3$ and $h_o/D \approx 0.2$ are obtained from Fig. 2 for this condition. Fig. 6 shows that h is slightly greater than h_s at the inlet. The profile at $L/D = 131$ shows that the liquid height behind the slug S1 is approximately equal to h_o. For these flow conditions, slugs formed at $L/D > 98$ are detected from the pressure trace. The h/D characterizing slugs is small because of the large amount of aeration.

The differences between the formation processes for $Fr > 1$ and for $Fr < 1$ are seen in Fig. 6. The profile at $L/D = 98$ shows that the replenishment of liquid after a slug has passed is accomplished by a bore of height h_s moving downstream. (The wave labeled as HJ1 in Fig. 6

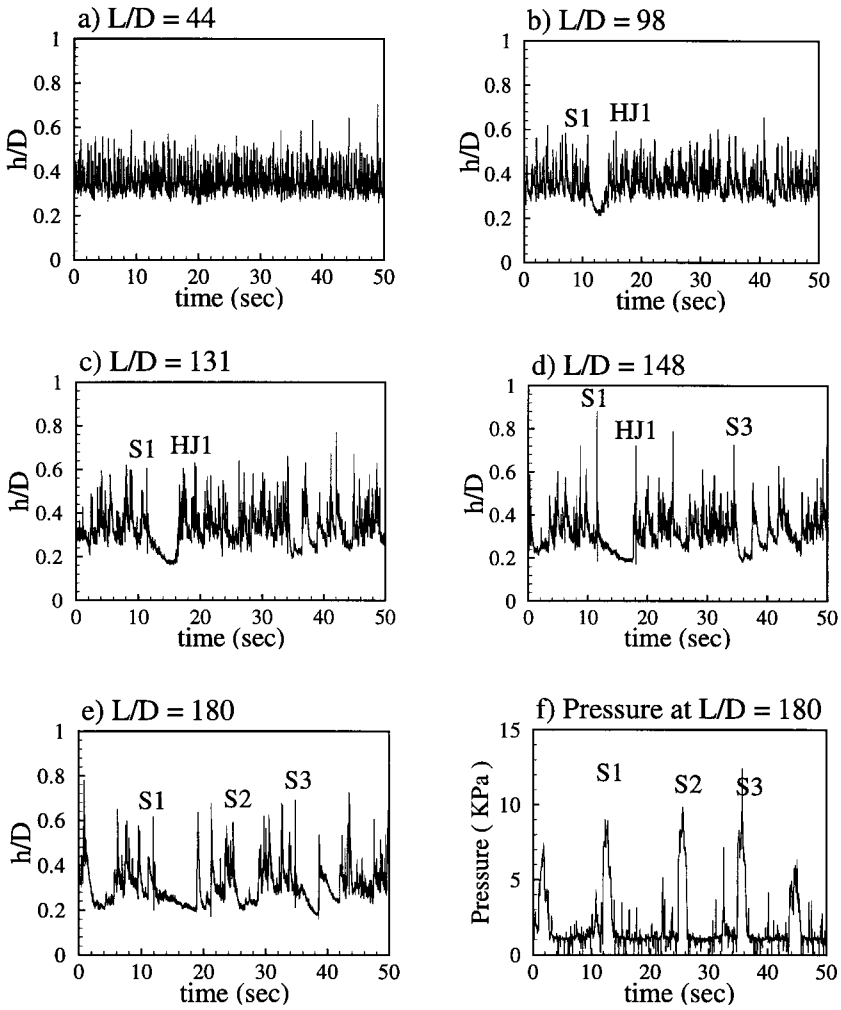

Fig. 6. Liquid holdup measurements and pressure measurement for $U_{SG} = 5.5$ m/s, $U_{SL} = 0.23$ m/s. Symbols S1, S2, S3 indicate slugs. Symbol HJ indicates a hydraulic jump.

represents a bore that developed as a result of the formation of the slug labeled as S1). Furthermore, the formation of slugs for $Fr > 1$ is much more irregular than for $Fr<1$. There is a large range of L/D at which slugs are formed and a large range of time intervals separating successive slugs.

At very high liquid flows, above curve B (zone III) in Fig. 4, slugs appear close to the entry and the formation is strongly affected by large amplitude waves created at the inlet. The outcome of these disturbances is influenced by the amount of liquid in the beginning portion of the pipeline at any given time. If a large amount of liquid is present in this region of the pipe, conditions are more favorable for the accumulation of liquid by a large amplitude disturbance and, thus, the formation of a slug. Consequently, only a fraction of the disturbances created near the inlet form slugs within zone III. The waves at the entry evolve into slugs by a process

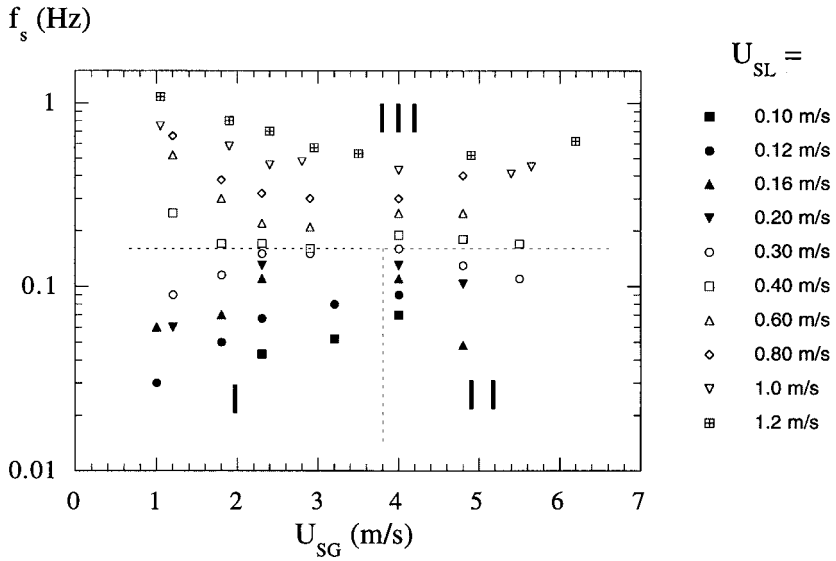

Fig. 7. Frequency of slugging, f_s as a function of U_{SG} and U_{SL}.

which is not easily identified. When slugs form at $L/D >$ Ca. 40, an instability almost always formed a slug. Curve B is defined as the boundary between zone I and III.

Fig. 7 gives data for the frequency of slugging. Three zones are identified. Within zone I, the frequency increases both with increasing superficial gas and liquid velocities. In zone II, the frequency decreases with U_{SG} and increases with U_{SL}. Zone III represents conditions for which slugs are formed at $L/D<$Ca. 40. For the most part, these are for $Fr > 1$. The results in zone III are similar to what has been found in smaller pipes by Gregory and Scott (1969), Taitel and Dukler (1977) and Heywood and Richardson (1979).

5. Slug formation within zone I

Wave spectra at different locations along the pipeline are given in Fig. 8 for similar conditions to those represented in Fig. 5. The spectral density functions, $\phi(f)$, are normalized with the mean square of the wave height fluctuations, ψ^2. High frequency waves are generated near the inlet. Energy becomes concentrated in waves with $f = 10$–12 Hz at $L/D = 21.5$. As already shown by Fan et al. (1993a, 1993b), these waves grow and bifurcate, as seen in the spectrum at $L/D = 49.1$. Fan et al. point out that the behavior of the 5 Hz waves that result from this bifurcation depends on the height of the stratified flow. They can eventually decay, tumble, or grow to touch the top of the pipe. For the conditions shown in Fig. 8, the height is large enough that waves evolve into slugs.

The formation of a slug at $U_{SG} = 1.8$ m/s and $U_{SL} = 0.12$ m/s in a pipe with $D = 7.63$ cm is shown in Fig. 9, which gives 10 sequential frames obtained with a high speed video camera. The time between frames is 1/30 s. The flow is right to left and a pipe length of 0.5 m is shown. Three wave crests, 16–20 cm apart, are observed in Fig. 9a. This corresponds to the spectrum at $L/D =$

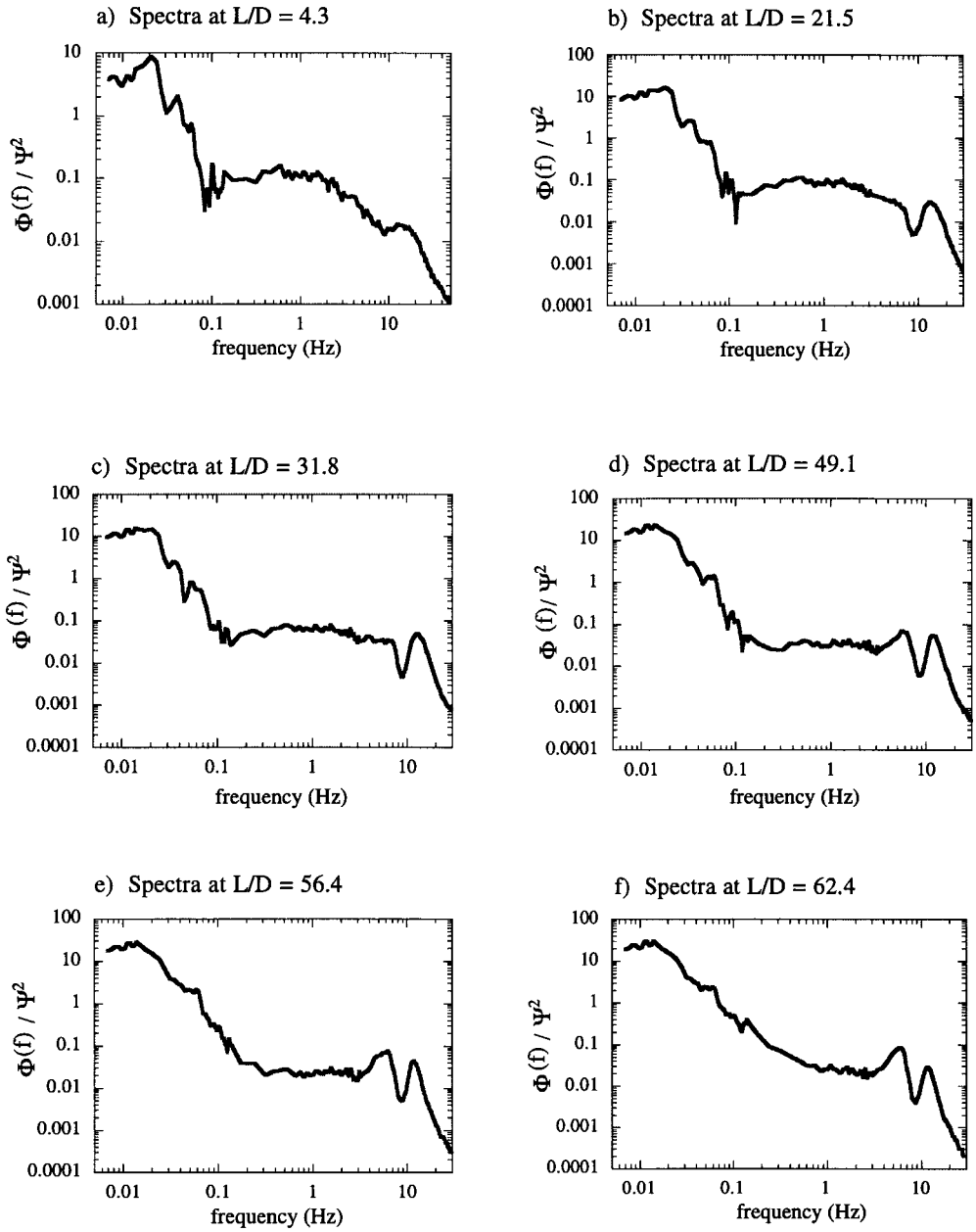

Fig. 8. Wave spectra for slug flow condition at $U_{SG} = 1.0$ m/s, $U_{SL} = 0.16$ m/s.

56 shown in Fig. 8 and the waves correspond to the 5 Hz peak. The wave velocity is, thus, approximately 0.9 m/s. The third wave from the left in Fig. 9a becomes unstable as it propagates downstream. It grows to form a slug in frame *h*. The liquid behind the slug decreases to h_o. The waves immediately behind the slug decay because they are propagating over a thinner layer. The pipe length shown in Fig. 9 is too small to observe the backward moving depression wave.

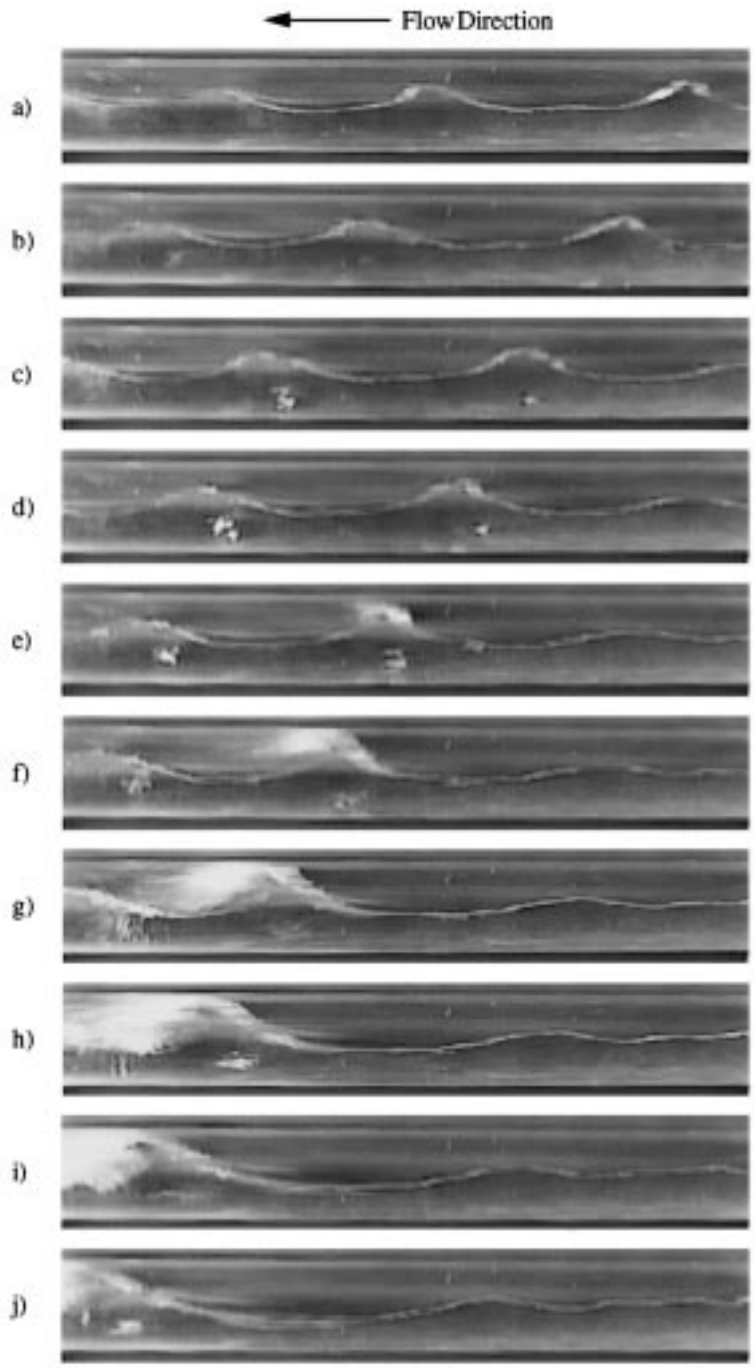

Fig. 9. Video images of slug formation within zone I.

Fig. 8 shows that, at upstream pipe locations where no slugs are observed, a considerable fraction of the wave energy is contained in frequencies that roughly correspond to the frequency of slugging for this flow condition, $f_s \approx 0.05$–0.06 Hz. The relative contribution of these low frequency disturbances to the total wave energy is determined by calculating the cumulative energy spectrum, $E(f_n)$, defined as

$$E(f_n) = \frac{\sum_{i=1}^{i=n} f_i \phi(f_i)}{\psi^2}. \tag{13}$$

Fig. 10 presents measurements of $E(f_n)$ for two liquid flows at $U_{SG} = 1.0$ m/s. Fig. 10a

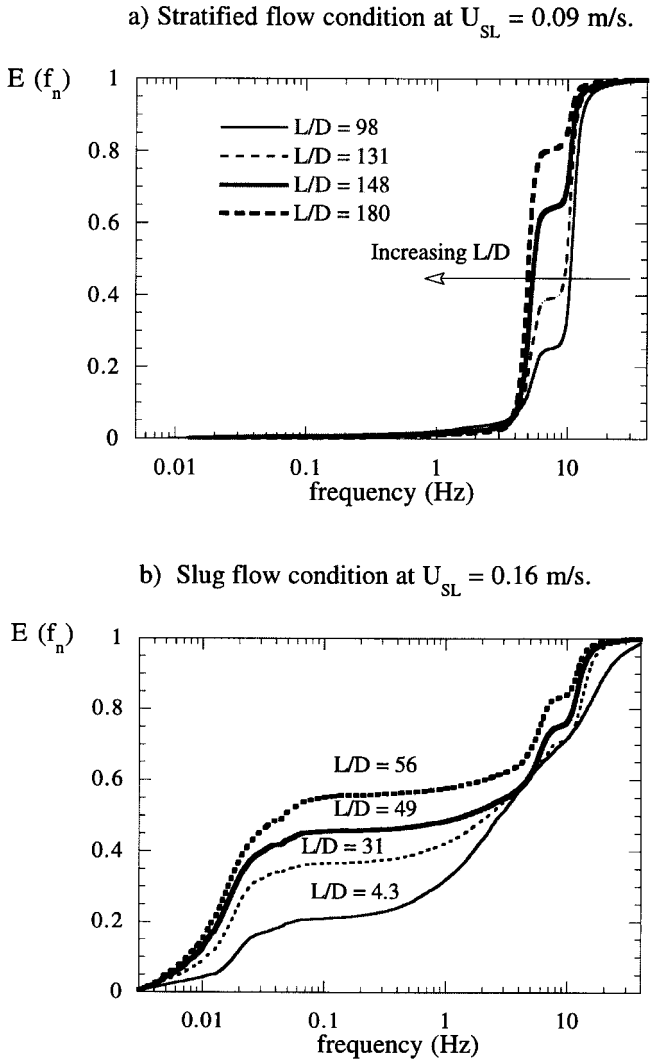

Fig. 10. $E(f_n)$ for two liquid flows at $U_{SG} = 1.2$ m/s.

represents a situation, $U_{SL} = 0.09$ m/s, for which no slugs appeared in the pipeline. At $L/D =$ 98 most of the energy is contained in waves with frequencies of 10–12 Hz. The contribution from waves of 5–6 Hz increases with increasing L/D until at $L/D = 180$ about 75% of the energy is contained in waves in the frequency range 5–6 Hz and 5% of the energy is found in waves with frequencies less than 5–6 Hz. If the liquid flow is increased, the mean height of the liquid layer increases until a height is reached at which the interfacial waves become unstable.

Fig. 10b presents cumulative energy spectra at $L/D = 4.3$, 31, 49, and 56 for the conditions represented by Fig. 5. Slugs were not observed at locations upstream of $L/D = 62$. Yet, a significant fraction of energy is contained at frequencies corresponding to the frequency of slugging, 0.05–0.06 Hz. It is of interest to explore the origin of these long wavelength waves and their role in the initiation of slugs.

The correlation coefficient $\rho_{12}(\tau)$ for a given time delay τ between wave height profiles at two different pipe locations is defined as

$$\rho_{12}(\tau) = \frac{E\left[h_1(\tau)^* h_2(t+\tau)\right]}{\sigma_1 \sigma_2} - \frac{\mu_1 \mu_2}{\sigma_1 \sigma_2} \tag{14}$$

where h_1 is the upstream liquid height, h_2, the downstream height, σ_1, σ_2, the standard deviations, μ_1,μ_2, the means. If a wave is translating downstream between two probes, the time delay τ for which a maximum occurs is positive. Fig. 11 shows that the maximum in the correlation function is at a negative value of τ, when the wave height profiles at $L/D = 12$ and 44 in Fig. 5 are used to determine $\rho_{12}(\tau)$. In this case, the upstream wave height profile lags the downstream wave height profile suggesting that a low frequency, long wavelength wave is translating upstream, rather than downstream.

Fig. 12 shows measurements of the liquid height at $L/D = 49$, 62, and 110 for $U_{SG} = 1.0$ m/s and $U_{SL} = 0.16$ m/s over a period of 40 s. The stability height, h_s, equals 0.6 for this condition. Two slugs are indicated at $L/D = 110$, one at $t = 370$ s and another at $t = 388$ s. Both of these

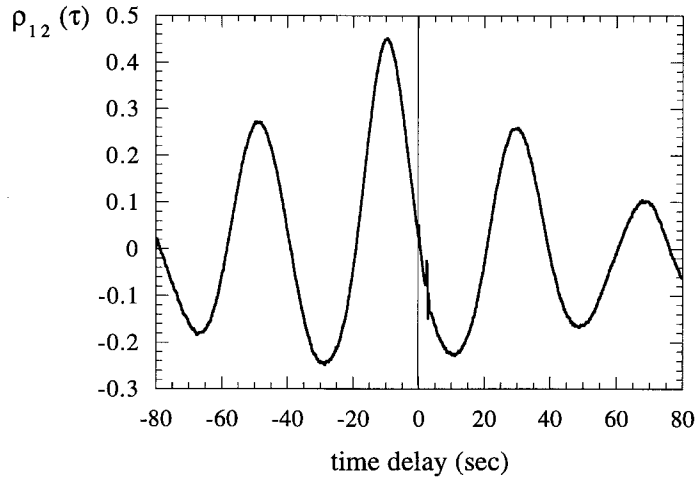

Fig. 11. Cross correlation function between wave height profiles at $L/D = 12$ and 44 for $U_{SG} = 1.0$ m/s, $U_{SL} = 0.16$ m/s.

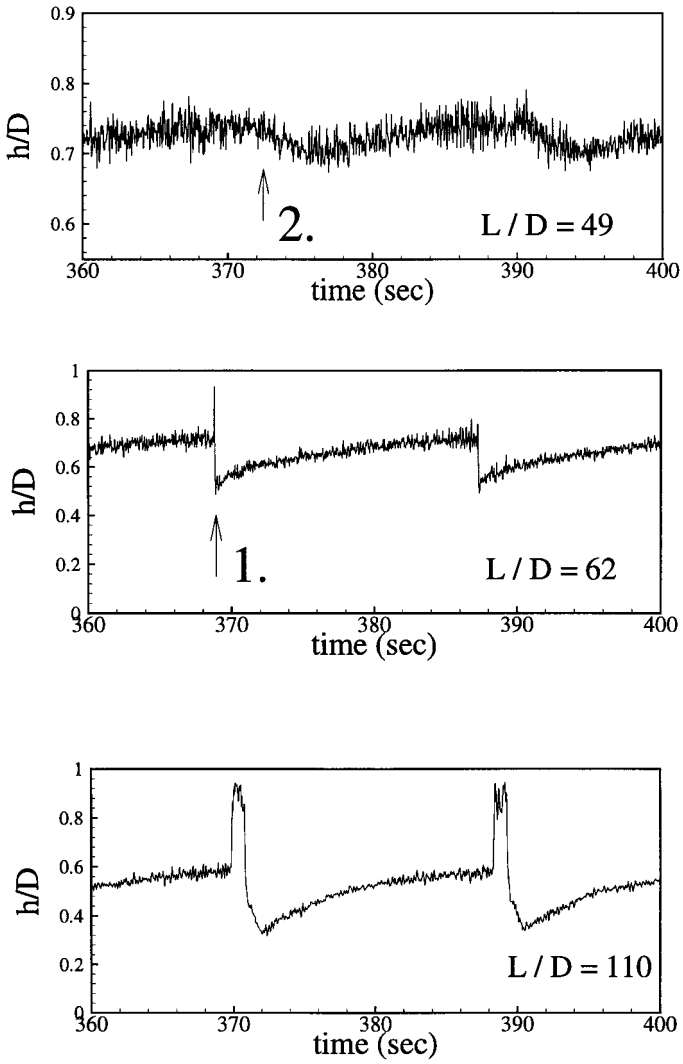

Fig. 12. Liquid holdup measurements for $U_{SG} = 1.0$ m/s, $U_{SL} = 0.18$ m/s illustrating the motion of a depression wave.

slugs were initiated from interfacial waves between $L/D = 49$ and 62. The first slug was initiated just upstream of $L/D = 62$ at $t = 369$ s, as indicated by the arrow labeled as 1. The liquid height remained at an approximately constant value of $h/D \approx 0.74$ at $L/D = 49$ over the time period of 366–372 s. Three seconds after the slug forms close to $L/D = 62$, the liquid layer height at $L/D = 49$ is depressed. The time at which the probe at $L/D = 49$ detects the depression wave associated with the formation of a slug is denoted by the arrow labeled as 2. The liquid heights at $L/D = 49$ and 62 increase over the time period 380 to 388 s until the liquid height is thick enough to produce another instability at $t = 388$ s. The gravity wave depresses the liquid layer at $L/D = 49$ just enough, so that no unstable waves are produced. The low frequency waves indicated by the frequency spectra in Fig. 8 and by the cross

correlation function in Fig. 11 are, therefore, associated with the formation of a slug when the flow of liquid is subcritical. The waves responsible for the initiation of a slug have frequencies of 5–6 Hz. The notion that the frequency of slugging is one-half of the frequency of the unstable waves responsible for slug initiation, presented by Tronconi (1990), does not appear to be consistent with these experimental data.

The shallow water Eqs. (10) and (11), have been solved to determine the interval between slugs. If the origin at $x = x_i$ is a perfect reflector, the boundary conditions would be $dh/dx = 0$ and a fixed volumetric flow rate, $q = U_{SL}A$, or $u_i = q/A_{L_i}$. These boundary conditions would allow h at the inlet to vary with time. Experiments showed a very small variation, so a boundary condition of a fixed A_{L_i} and a fixed u_i was chosen at $x = x_i$ to simplify the calculations. A non-linear partial differential equation solver in IMSL libraries was used. The initial condition for the solution was obtained from experimental observations, and is given by the liquid layer profile in Fig. 13a. In accordance with Fig. 12, the discontinuity is placed at $L/D = 60$. The liquid height downstream of $L/D = 60$ is taken to be $h/D \approx 0.35$. The liquid velocity within this layer is assumed to be zero. The liquid layer upstream of the discontinuity varies in height from $h/D \approx 0.78$ at $L/D = 0$ to $h/D \approx 0.70$ at $L/D = 60$. The liquid velocity within the stratified flow is $u = U_{SL}A/A_L$. Since the flow is subcritical, a depression wave moves upstream of $L/D = 60$. Fig. 13a gives the solution during the time period for which the depression wave propagates upstream. The wave front moves closer to the inlet as time proceeds. When it reaches the inlet, at approximately 10 s, the liquid height is rebuilt as shown by the height profiles in Fig. 13b. The liquid layer returns to the initial condition after approximately 17 s. This time agrees with the time interval between slugs in Fig. 12.

Fig. 14 compares the experimental values for the frequency of slugging for case I, given in Fig. 7, with those calculated by the above procedure. In accordance with (10), the parameter $t_s u_S/L_D$ is plotted as a function of Fr, where t_s is the time interval between slugs ($t_s = 1/f_s$) and u_S is the liquid velocity corresponding to the instability condition, h_s. The filled symbols represent values obtained from the solution of the shallow water equations. The open symbols are obtained from experimental observations. Good agreement is noted. A critical parameter that appears in this analysis is the pipe length, L_D, required to generate an unstable wave pattern. The bars in Fig. 14 reflect the error in estimating the value of L_D. Fig. 15 shows the variation of the mean values of L_D with the flow velocities, U_{SG} and U_{SL}. This parameter was estimated by measuring the liquid holdup at various locations in the pipeline for several different flow conditions and estimating the probe at which a slug is first observed. Each mean value in Fig. 15 is based on an ensemble of at least 100 slugs. The length L_D depends on how rapidly waves develop in the flow direction. Since this could depend on disturbances introduced at the inlet, the frequency of slugging in zone I could be affected by the construction of the inlet.

6. Slug formation within zone II

At the onset to slugging for horizontal air–water flows at $U_{SG} > 4$ m/s, Lin and Hanratty (1986a, 1986b) observed that the gas–liquid interface is dominated by irregular waves. The

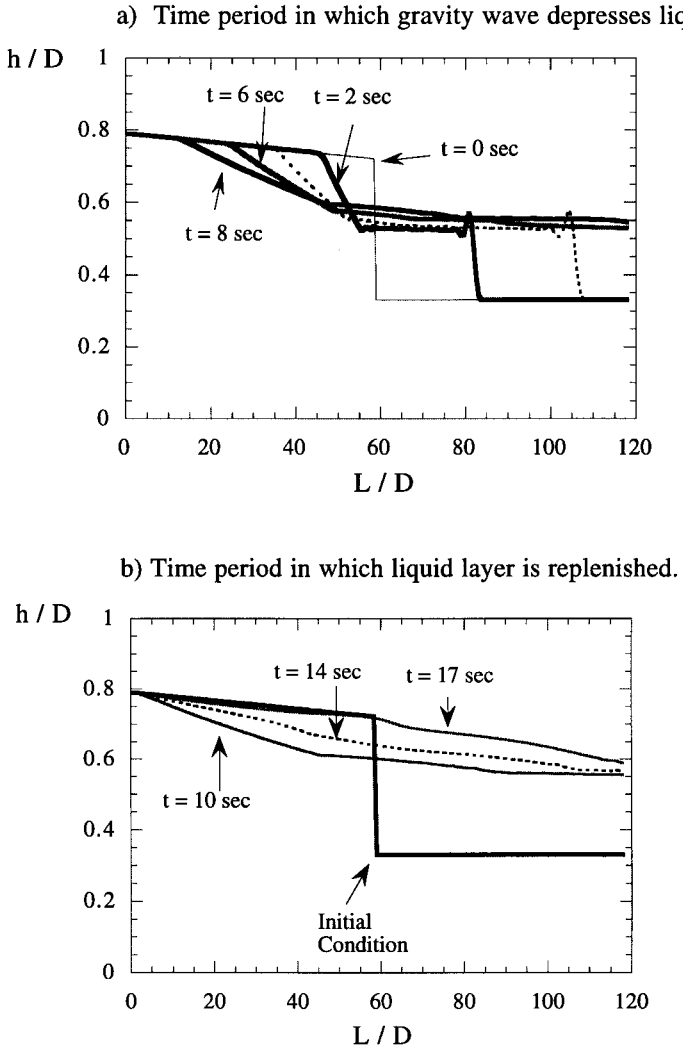

Fig. 13. Solution of the shallow water equations for the slug flow condition at $U_{SG} = 1.0$ m/s, $U_{SL} = 0.18$ m/s.

regular $f = 5$ Hz waves which are responsible for generating a slug at low gas flows rapidly form close to the inlet at high gas flows. Fig. 16 shows cumulative energy spectra $E(f_n)$, defined by (13), of a stratified flow at several pipe locations at $U_{SG} = 5.5$ m/s and $U_{SL} = 0.20$ m/s. This value of U_{SL} is slightly less than that of Fig. 6 and represents the onset to slug flow for $U_{SG} = 5.5$ m/s. For this flow condition, $h_s/D = 0.3$, $Fr = 1.1$. The cumulative energy spectra at $L/D = 12$ in Fig. 16 represents the energy spectra of a gas–liquid interface that is dominated by 5–6 Hz waves. The height of the stratified flow at $L/D = 12$ is not thick enough for the $f = 5$ Hz waves to initiate slugs. These waves grow in amplitude until their limiting height is reached and roll waves form when they break. Lin and Hanratty (1986a, 1986b), Andritsos et al. (1989), Fan et al. (1993a, 1993b) observed

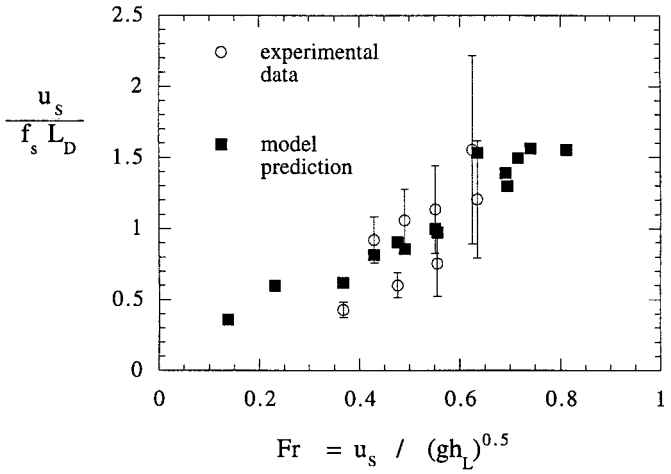

Fig. 14. Comparison of predicted and experimental slug frequencies within zone I.

that the resulting wave pattern is irregular. Fig. 17 compares the cross correlation functions for wave patterns at the transition to slug flow from two probes separated by a distance of 15.2 cm at $L/D = 138$, for a regular wave pattern, observed for $U_{SG} = 3.0$ m/s and $U_{SL} = 0.08$ m/s, and for an irregular wave pattern, observed for $U_{SG} = 5.0$ m/s and $U_{SL} = 0.12$ m/s. Since the peaks and troughs of the cross correlation function in Fig. 17a are separated by 0.2 s for a number of cycles, this wave pattern is approximately periodic. The only dominant peak in the cross correlation function in Fig. 17b occurs at 0.2 s, which equals the quotient of the probe separation and the average wave velocity. No regularity is indicated. The irregular waves have a range of wave velocities so they can overtake one another. The cumulative spectra in Fig. 16, suggest that wave coalescence results in a decrease in the median frequency, as the waves translate downstream.

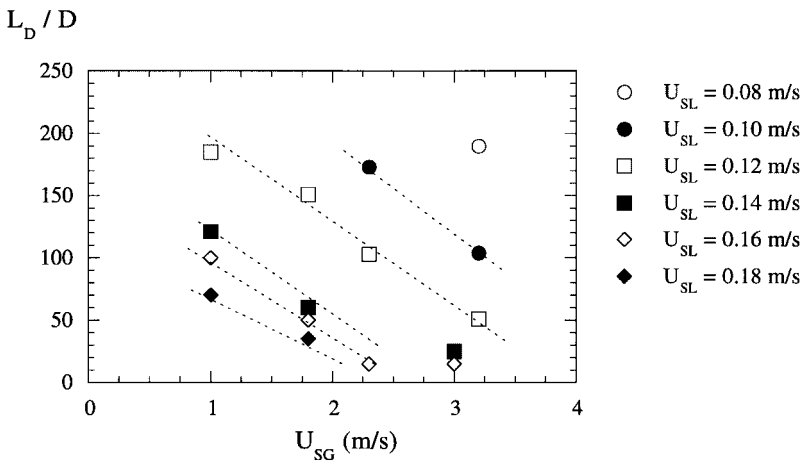

Fig. 15. Variation of L_D/D with U_{SG} and U_{SL}.

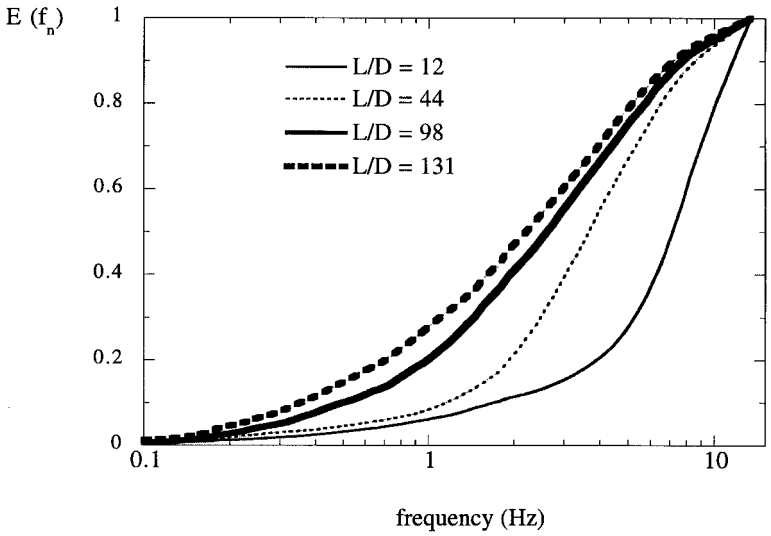

Fig. 16. Cumulative wave spectra for $U_{SG} = 5.5$ m/s, $U_{SL} = 0.20$ m/s.

An example of the initiation of a slug by the coalescence of roll waves is presented in Fig. 18, which has nine sequential frames obtained with a high speed video camera. The time between frames is 1/30 s. The flow is right to left and a pipe length of 0.5 m is shown. Three roll waves are observed in Fig. 18a. The roll waves are characterized by a steep front and a gradually sloping tail. A large roll wave enters the frame in b and c. As this wave translates downstream, a faster moving roll wave overtakes it in d, e, and f. Frames g, h, and i show that this coalescence results in a larger roll wave. In this example, the coalescence produces a wave whose height is large enough to become unstable. For $U_{SG} \leq 4.0$ m/s, slugs initiate by the mechanism illustrated in Fig. 9. For $U_{SG} \geq 4.0$ m/s, wave coalescence, shown in Fig. 18, is responsible for slug initiation.

The liquid holdup measurements in Fig. 6 for $u = 0.61$ m/s and $Fr = 1.15$ indicate that slug formation occurs randomly in space and time. No slugs are observed at $L/D = 44$. The wave pattern at this location is similar to that shown by the wave spectrum at $L/D = 131$ in Fig. 16; roll waves are present. Three slugs are labeled as S1, S2, and S3 in Fig. 6 on the pressure trace at $L/D = 185$ and on the liquid holdup measurement at $L/D = 180$. The slug labeled as S1 forms at a location between $L/D = 44$ and 98. As this slug passes the probe at $L/D = 98$, the liquid height decreases to $h_o/D = 0.2$. Since $Fr > 1$, a hydraulic jump, labeled as HJ1, replenishes the liquid back to the height h_s, a short time later. As this hydraulic jump translates downstream, the length of the unstable wave pattern upstream of the slug increases. Consequently, the probability of forming another slug increases. Slug S2 is observed to form between $L/D = 148$ and 180. Slug S3 forms at a location between $L/D = 131$ and 148. For case II, therefore, a length of pipe is required to develop an unstable roll wave pattern. Beyond this location, there is a probability of forming a slug at any location at which the liquid height is equal to h_s. Fig. 19 shows 100 s of the pressure signal at $L/D = 185$ for $U_{SG} = 5.5$ m/s and $U_{SL} = 0.28$ m/s. The peaks, which indicate the passage of a slug, are not periodic. The formation process is clearly stochastic.

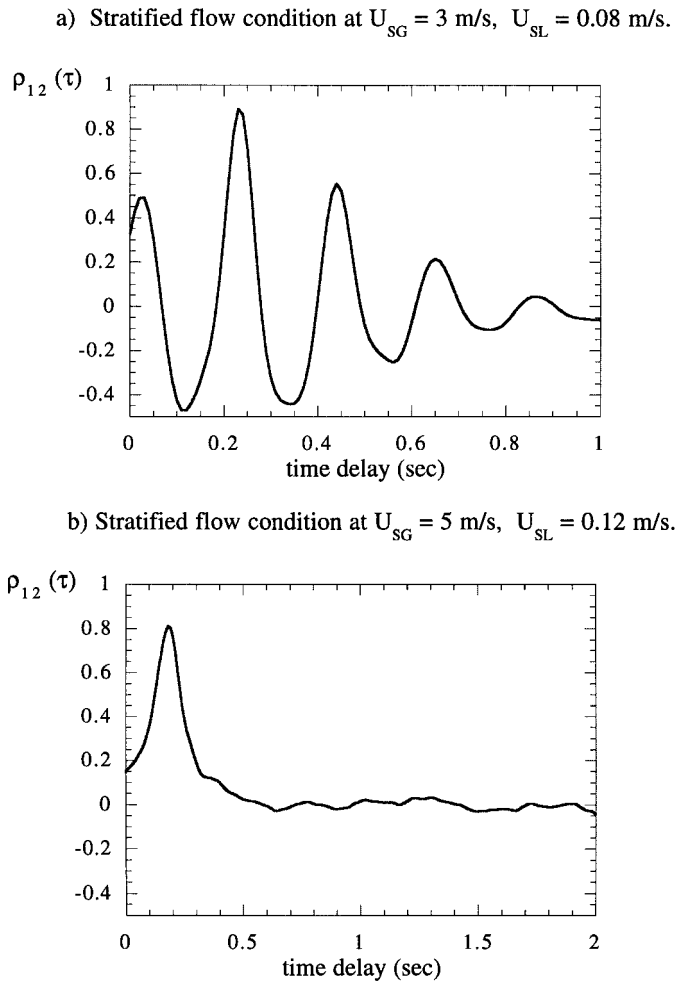

Fig. 17. Cross correlation functions for regular and irregular waves.

Fig. 20 presents a schematic which describes a probabilistic model for the formation of slugs for case II. A stratified flow exists at the beginning of the pipe of length L_D over which wave development occurs. Beyond L_D, an unstable irregular wave pattern exists over the length L_U. It is assumed that it is equally probable for roll waves to coalesce to form a slug at all locations between L_D and L_U. After a slug forms, it translates downstream, rapidly picks up liquid at the front, and sheds liquid at the tail to form a stratified flow of height h_o. Since $Fr > 1$, a hydraulic jump forms at the location at which the slug formed; it moves downstream with velocity C_{jump} and restores the liquid to height h_s. The probability of forming a slug between x and $(x + dx)$ and between t and $(t + \Delta t)$ is defined as N, which is taken to be independent of x. The probability of forming a slug between locations L_D and $L_D + L_U(t)$ over the interval Δt is then given as

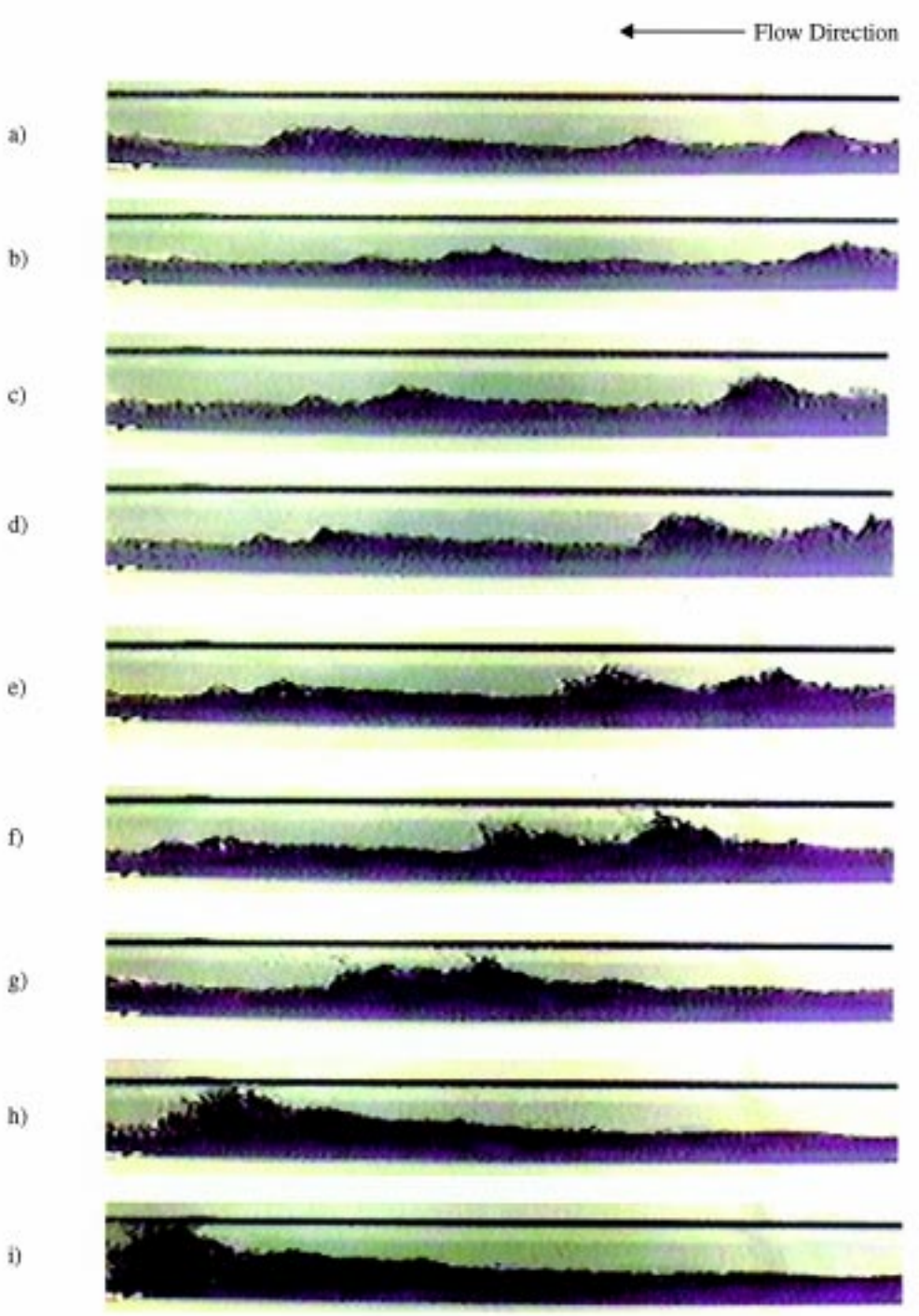

Fig. 18. Video images illustrating the formation of a slug within zone II due to coalescence of roll waves.

$$\Delta t P(t) = \Delta t \int_0^{L_U(t)} N \, \mathrm{d}x \; = \Delta t N L_U(t) \tag{15}$$

where N has the units of reciprocal time and reciprocal length. The length of the unstable wavy stratified flow increases with time at a rate given by

$$L_U(t) = L_f + C_{\text{jump}} \Delta t \tag{16}$$

where $L_f + L_D$ is the pipe location at which a previous slug was formed at $t = 0$. The introduction of Eq. (16) into (15) gives the following expression:

$$\Delta t P(t) = N\big(L_f + C_{\text{jump}} t\big)\Delta t \tag{17}$$

The randomness of the slugging process is modeled through the use of random number generators. At $t = t + \Delta t$, a random number R_{i} between 0 and 1 is selected and compared with the value of $\Delta t P(t)$, obtained by Eq. (17). If $R_{\text{i}} > \Delta t P(t)$, a slug does not form. The time is incremented by Δt, L_U is increased by an amount $C_{\text{jump}} \Delta t$, another random number is generated, and the calculation is repeated until $R_{\text{i}} < \Delta t P(t)$. If $R_{\text{i}} < \Delta t P(t)$, a slug has formed at some location along L_U. A second random number generator is then used to determine where, along L_U, this occurred. This becomes the new value of L_f. The algorithm is repeated to generate an ensemble of time intervals between the formation of slugs and an ensemble of pipe locations beyond L_D at which the slugs form. The constant N is chosen so that the mean value of the ensemble of time intervals between slug formation obtained by the above algorithm is consistent with the slug frequency that was determined by experiment.

Velocity C_{jump} is determined analytically by applying conservation of mass between stations 1 and 2 in Fig. 20 in a reference frame moving with the hydraulic jump

$$\big(C_{\text{jump}} - u_{\text{s}}\big)A_{\text{s}} = \big(C_{\text{jump}} - u_{\text{o}}\big)A_{\text{o}}, \tag{18}$$

where A_{s} and A_{o} are the cross sectional areas occupied by liquid of heights h_{s} and h_{o}. A value of u_{o} is determined from equations (Andritsos and Hanratty, 1987) that describes an equilibrium stratified flow of height h_{o} in the presence of a gas velocity $U_{\text{o}} = U_{\text{SG}} A/(A - A_{\text{o}})$.

The probabilistic approach outlined above is compared with measurements of the distribution of time intervals between slug formation in Fig. 21 for two different flow conditions. The thin line in Fig. 21a represents the distribution of time intervals between pressure pulses, associated with 472 slugs, at $U_{\text{SG}} = 5.5$ m/s and $U_{\text{SL}} = 0.28$ m/s. The slug frequency for this flow condition is 0.11 Hz. The mean value of the distribution in Fig. 21a is 8.9 s. For $N = 0.0092$, the predicted distribution has the same expected value. The shapes of the calculated and measured distributions are similar. However, the calculated maximum is lower than the measured value. Fig. 21b compares computed and experimental spectra for $U_{\text{SG}} = 5.5$ m/s and $U_{\text{SL}} = 0.40$ m/s. A value of $N = 0.0153$ is selected so that computed and experimental distributions have the same mean slug frequency, 0.17 Hz.

Reasonable agreement between the experimental and computed probability distributions are obtained for values of N shown in Fig. 22. This figure indicates that the probability constant N is sensitive to u, equal to $U_{\text{SL}} A/A_{\text{s}}$, and relatively insensitive to changes in U_{SG}. Fig. 23 gives values of L_D that were used in the stochastic formulation. Slugs form close to the outlet at

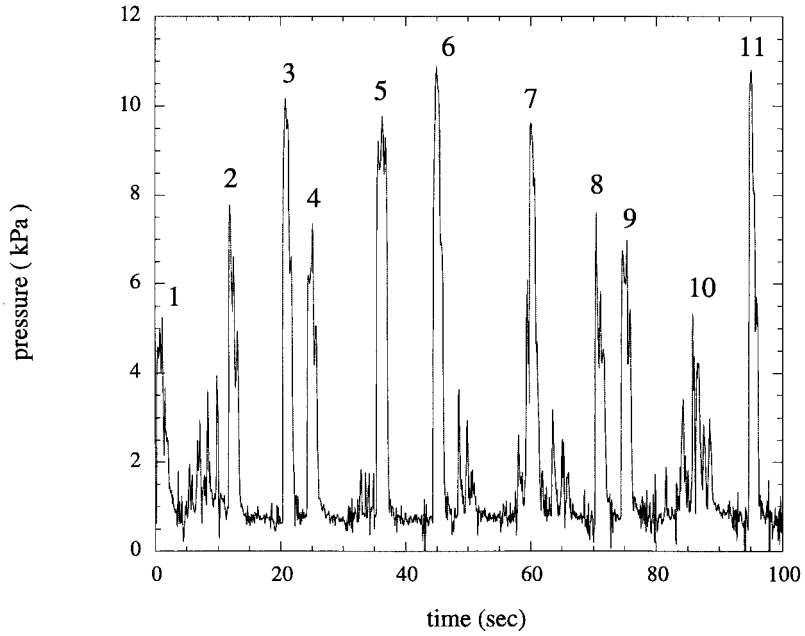

Fig. 19. Pressure measurement at $U_{SG} = 5.5$ m/s, $U_{SL} = 0.28$ m/s.

liquid velocities close to the stratified-slug transition (curve A in Fig. 4). As u increases, slugs are observed closer to the inlet. Results for N in Fig. 22 are shown for flow conditions for which the slugs were observed at $L_D/D \leq 125$. For flow conditions such that $L_D/D \geq 125$, the length $L_D + L_U$ may equal the total pipe length, suggesting that if the pipe were longer, f_s would be larger. The values of N needed to compute frequencies consistent with the experimental slug frequencies for these flow conditions could, therefore, be lower than the values plotted in Fig. 22.

7. Discussion

Measurements are characterized, according to the mechanism of slug formation, by the sub-regimes shown in Fig. 4. The boundaries are defined by the Froude number and the location in

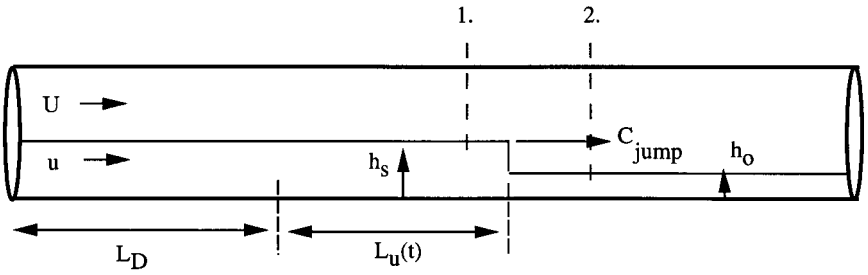

Fig. 20. Schematic of the probabilistic model for case II.

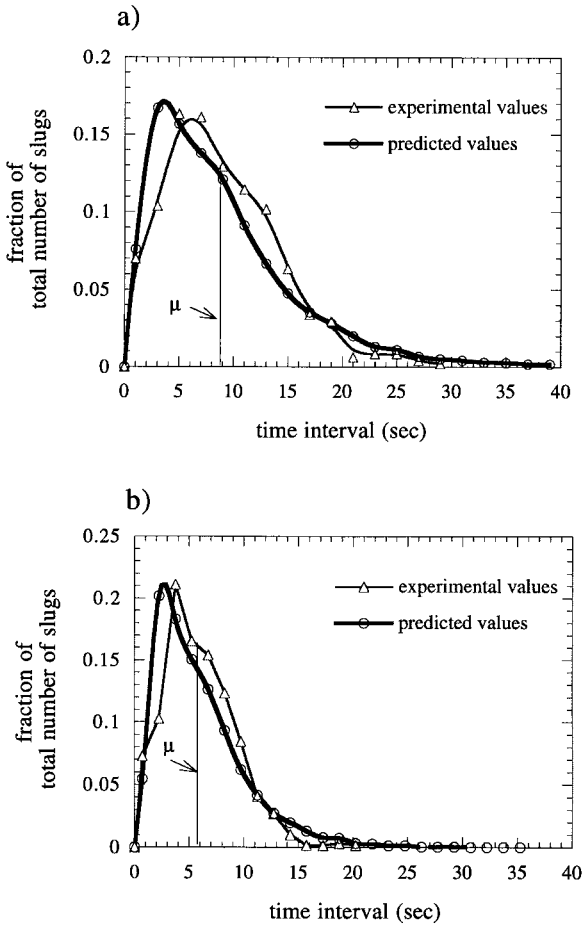

Fig. 21. Comparison between experimental and model distributions for the time interval between slugs: (a) $U_{SG} = 5.5$ m/s, $U_{SL} = 0.28$ m/s; (b) $U_{SG} = 5.5$ m/s, $U_{SL} = 0.40$ m/s).

the pipeline where slugs are observed to form. For low gas and liquid velocities, the liquid flow is characterized by subcritical flows ($Fr<1$) and a deterministic model for the slug frequency is proposed which takes into account an upstream translation of a gravity wave associated with the formation of a slug. This wave depresses the liquid below the critical liquid layer height, h_s, needed to initiate a slug; the next slug is formed when this depleted liquid is replenished. For $U_{SG} > 4$ m/s, the formation of slugs, in the experiments described in this paper, should be interpreted as a stochastic process. Measurements and photographs suggest that a model should take into account the probability of forming a slug over a patch of an unstable wavy stratified flow, as a consequence of roll wave coalescence. For $U_{SG} > 4$ m/s, the flow of liquid is supercritical ($Fr > 1$), so that the liquid is rebuilt to the height h_s by a hydraulic jump after the formation of a slug.

The most widely used model for predicting the slug frequency is that proposed by Taitel and Dukler (1977). Since this deterministic model considers the frequency to be related to the liquid

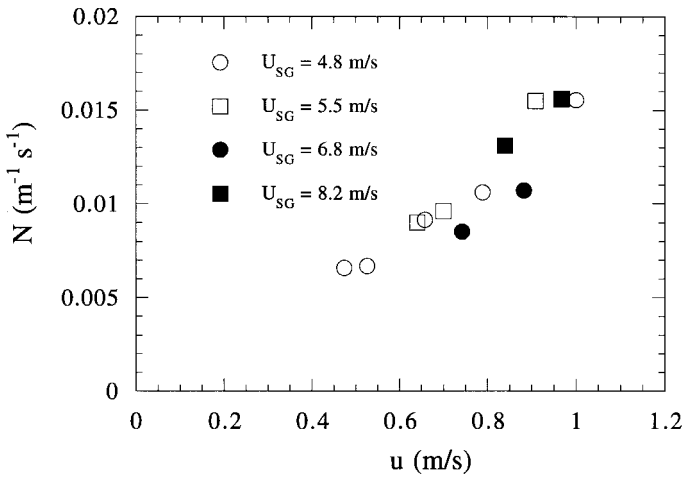

Fig. 22. Variation of the probability constant N with u.

replenishment just downstream of the pipe location at which a slug is formed, one could consider it to represent supercritical flows. However, measurements presented here indicate that, for supercritical flows in which slugs form far downstream of the inlet, the frequency is related to the probability that a slug forms from the coalescence of roll waves along a length of unstable wavy stratified flow. The notion that the slug frequency is proportional to the frequency of the unstable waves, as hypothesized by Tronconi (1990), is not supported by the measurements and photographs presented in this work.

Critical parameters which evolve out of this analysis are h_s, h_o, and L_D. Taitel and Dukler (1977) modeled the rebuilding of the liquid layer from a level given by h_s back to an equilibrium height h_e that would exist for the given flow conditions. Our results suggest that the liquid rebuilds from a level h_o, dictated by the necessary conditions for the existence of slug (Ruder et al., 1988; Woods and Hanratty, 1996), to the level h_s. Furthermore, results indicate

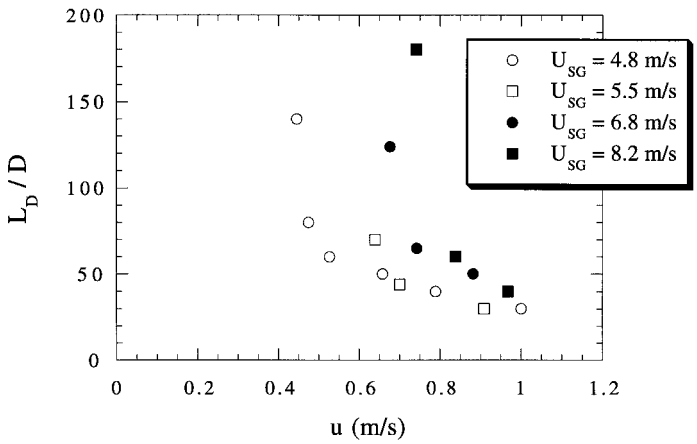

Fig. 23. Variation of L_D/D with u for case II flows.

that the pipe length required to produce an unstable wavy stratified flow, L_D, strongly influences the frequency of slugging. The prediction of L_D is complicated by the possible influence of the construction of the gas–liquid mixer. Fig. 24 shows the root mean square of the liquid holdup measurements as a function of distance from the inlet, L/D, for six different liquid velocities at $U_{SG} = 2.3$ m/s. For this gas velocity, the transition to slug flow occurs at $U_{SL} = 0.10$ m/s. Consequently, the measurements in Fig. 24 for $U_{SL}<0.10$ m/s denote the rms of wave height fluctuations, $h' = h_L - \langle h_L \rangle$. For each of these flows, $\sqrt{\langle h^2 \rangle}$ increases with L/D, indicating that the waves grow in amplitude with distance. The parameter $\sqrt{\langle h'^2 \rangle}$ achieves a constant value at the end of the pipeline at $U_{SL} = 0.04$ m/s, suggesting that the waves have saturated. For $U_{SL} = 0.06$, 0.08, and 0.10 m/s, $\sqrt{\langle h'^2 \rangle}$ increases over the entire pipeline. For $U_{SL} = 0.10$ m/s, the root-mean square of the wave amplitude at $L/D = 180$ is large enough, and the liquid layer height is thick enough for instabilities to occur. For $U_{SL} > 0.10$ m/s, the waves necessary to produce slugs are generated closer to the inlet. The horizontal line labeled as 1 in Fig. 24 denotes the approximate value of $\sqrt{\langle h'^2 \rangle}$ needed to produce slugging. For data above this line, slugs are observed at the indicated L/D. If a longer pipeline was used, Fig. 24 suggests that slugs might be observed at $U_{SL} = 0.06$ and 0.08 m/s, since $\sqrt{\langle h'^2 \rangle}$ does not reach a constant value in the pipeline used in the experiments. As U_{SL} increases, the combination of air and water in the simple tee arrangement results in an increase in $\sqrt{\langle h'^2 \rangle}$ at $L/D = 4$. Thus, the value of L/D at which slugs are formed could be sensitive to the construction of the inlet.

It is well documented in the literature that parameters such as the pipe diameter, pipe inclination, and fluid properties have a strong influence upon the transition from a stratified flow to a slug flow. Consequently, the boundaries among zones I, II, and III in Fig. 4 are expected to be a function of these parameters. Shoham (1982) has shown that liquid velocities of $U_{SL} = 0.8$ to 1.0 m/s are needed to initiate slugging in a 5.1 cm diameter pipe declined at 1°. Gravity waves associated with zone I slugging would not be expected under such conditions, since the Froude number would be greater than unity. Conversely, slug flows are observed over a wider range of flow conditions for upflows. For a pipe inclination of 1°, the stratified flow

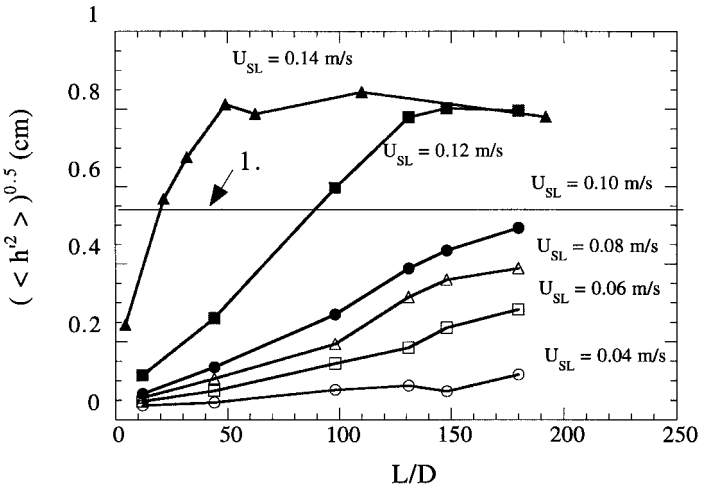

Fig. 24. Variation of the root-mean square of the wave height fluctuations, $\sqrt{\psi^2}$, with L/D at $U_{SG} = 2.3$ m/s.

region in a flow regime map shrinks to a very small bell-shaped region (Grolman et al., 1996). Thus, the range of slug flow conditions characterized by subcritical liquid flows would be expected to be large for upflows. For high viscosity liquids, the liquid velocity is lower than for water at a given U_{SG} and h/D. In these flows, zone I would extend over a wider range of conditions.

Acknowledgements

This work is supported by the Department of Energy under Grant DOE DEF 86ER 13556.

References

Andritsos, N., Hanratty, T.J., 1987. Influence of interfacial waves in stratified gas–liquid flows. AIChE J. 33, 444–454.

Andritsos, N., Williams, L., Hanratty, T.J., 1989. Effect of liquid viscosity on the stratified slug transition in horizontal pipe flow. Int. J. Multiphase Flow 15, 877–892.

Andreussi, P., Minervini, A., Paglianti, A., 1993. Mechanistic model of slug flow in near-horizontal pipes. AIChE J. 39, 1281–1291.

Bendikson, K.H., Esperal, M., 1992. Onset of slugging in horizontal gas–liquid pipe flow. Int. J. Multiphase Flow 18, 237–247.

Benjamin, T.B., 1968. Gravity currents and related phenomena. J. Fluid Mech. 31, 209–248.

Dukler, A.E., Hubbard, M.G., 1975. A model for gas–liquid slug flow in horizontal tubes. Ind. Eng. Chem. Fundam. 14, 337–347.

Dukler, A.E., Maron, D.M., Brauner, N., 1985. A physical model for predicting the minimum slug length. Int. J. of Multiphase Flow 40, 1379–1385.

Fan, Z., Lusseyran, F., Hanratty, T.J., 1993a. Initiation of slugs in horizontal gas–liquid flows. AIChE J. 39, 1741–1753.

Fan, Z., Ruder, Z., Hanratty, T.J., 1993b. Pressure profiles for slugs in horizontal pipelines. Int. J. Multiphase Flow 19, 421–437.

Gregory, G.A., Scott, D.A., 1969. Correlation of liquid slug velocity and frequency in horizontal cocurrent gas–liquid slug flow. AIChE J. 15, 933–935.

Grolman, E., Commandeur, N., de Baat, E., Fortuin, J., 1996. Wavy-to-slug flow transition in slightly inclined gas–liquid pipe flow. AIChE J. 42, 901–907.

Heywood, N.I., Richardson, J.F., 1979. Slug flow in air water mixtures in a horizontal pipe: determination of liquid holdup by Γ-ray absorption. Chem. Eng. Sci. 34, 17–30.

Hubbard, M.G., 1965. An analysis of horizontal gas liquid slug flow. PhD thesis, University of Houston.

Kokal, S.L., Stanislav, J.F., 1989. An experimental study of two-phase flow in slightly inclined pipes. Part II: Liquid holdup and pressure drop. Chem. Engng. Sci. 44, 681–693.

Lin, P.Y., Hanratty, T.J., 1986a. Prediction of the initiation of slugs with linear stability theory. Int. J. of Multiphase Flow 12, 79–98.

Lin, P.Y., Hanratty, T.J., 1986b. Detection of slug flow from pressure measurements. Int. J. of Multiphase Flow 13, 13–21.

Milne-Thomson, L.M., 1968. Theoretical Hydrodynamics, 5th ed. MacMillan Press, London.

Mishima, K., Ishii, M., 1980. Theoretical prediction of onset of horizontal slug flow. J. Fluids Eng., ASME Trans. 102, 441–445.

Nicholson, M.K., Aziz, K., Gregory, G.A., 1978. Intermittent two phase flow in horizontal pipes: predictive models. The Can. J. of Chemical Eng. 56, 653–663.

Nydal, O.J., Pintus, S., Andreussi, P., 1992. Statistical characterization of slug flow in horizontal pipes. Int. J. Multiphase Flow 18, 439–453.

Ruder, Z., Hanratty, P.J., Hanratty, T.J., 1988. Necessary conditions for the existence of stable slugs. Int. J. Multiphase Flow 15, 209–226.

Shoham, O., 1982. Flow pattern transitions and characterization in gas–liquid flow in horizontal pipes. Ph.D. thesis, Tel-Aviv University, Israel.

Stoker, J.J., 1957. Water Waves. Interscience, New York.

Taitel, Y., Dukler, A.E., 1976. A model for predicting flow regime transitions in horizontal and near horizontal gas–liquid flow. AIChE J. 22, 47–55.

Taitel, Y., Barnea, D., Dukler, A.E., 1980. Modeling flow pattern transitions for steady upward gas–liquid flow in vertical tubes. AIChE J. 3, 345–354.

Taitel, Y., Dukler, A.E., 1977. A model for slug frequency during gas–liquid flow in horizontal and near horizontal pipes. Int. J. Multiphase Flow 3, 585–596.

Tronconi, E., 1990. Prediction of slug frequency in horizontal two-phase slug flow. AIChE J. 36, 701–709.

Wallis, G.B., Dobbins, J.E., 1973. The onset of slugging in horizontal stratified air–water flow. Int. J. Multiphase Flow 1, 173–193.

Wu, H.L., Pots, B.F.M., Hollenburg, J.F., Merhoff, R., 1987. Flow pattern transitions in two-phase gas/condensate flow at high pressure in an 8-inch horizontal pipe. In: Proc. BHRA Conf, The Hague, The Netherlands, 13–21.

Woods, B.D., Hanratty, T.J., 1996. Relation of slug stability to shedding rate. Int. J. Multiphase Flow 22, 809–828.